



Test Beam Measurements with Pixel Telescopes

- Efficiency and Mechanical Stability -

Cora Fischer, Georg-August-Universität Göttingen, Germany

September 8, 2011



Abstract

The EUDET pixel telescope is designed for test beam operation. The energy and particles of a test beam are known and therefore allow a precise test of future detectors with the help of the EUDET telescope. The EUDET telescope can determine the performance of newly developed detectors concerning the spatial resolution. Measurements with test beams at CERN (pions, SPS storage ring) and DESY (electrons, DESY II) were performed without a tested pixel detector (DUT, Device Under Test). These measurements were made to study the spatial resolution, efficiency and noise rate of the telescope itself dependent on different threshold settings and energies of the impinging particles. The data taken from the SPS test beam were analyzed and the results for the mechanical stability of the telescope and the efficiency of the telescope sensors are presented here.

Contents

1	Introduction	3
2	Test Beam	3
2.1	DESY II	3
2.2	SPS	4
3	The EUDET Telescope	4
3.1	Experimental Setup	5
3.2	EUDAQ Software	5
3.3	EUTelescope analysis software	7
3.3.1	Conversion	7
3.3.2	Clustering	7
3.3.3	Hitmaker	7
3.3.4	Alignment	8
3.3.5	Track-Fitting	8
4	Measurement	9
4.1	Test Beam Measurement at the CERN SPS Storage Ring	9
4.2	Test Beam at DESY II	10
5	Results	10
5.1	CERN Test Beam	10
5.1.1	Alignment Parameters - Mechanical Stability	10
5.1.2	Efficiency	14
5.2	Common Result	15
6	Summary and Conclusion	16
A	Efficiency Calculation	18

1 Introduction

EUDET is an “Integrated Infrastructure Initiative” within the EU funded “6th framework programme” aimed at providing detector research and development (R&D) infrastructure towards a future linear collider or other particle physics experiments [1]. 29 institutes from 12 countries contribute to the EUDET project which is coordinated by DESY [2]. The access to the DESY test beam facility is part of the detector R&D infrastructure. JRA 1 (Joint Research Activity) is a subproject of EUDET and has the goal to improve the test beam infrastructure via a high-resolution pixel telescope that enables the study of precision tracking devices. This pixel telescope is the EUDET telescope¹. The telescope is a tool to measure the exact tracks of a test beam with very high precision. This measurements serve as a reference information when testing newly developed detector modules (DUTs). The pointing resolution is the resolution power concerning the prediction of a track at the position of the DUT. In order to be able to test a DUT the pointing resolution of the telescope should be better than the expected intrinsic resolution of the DUT. This requirement is fulfilled for the EUDET telescope. The measurements at the CERN and DESY test beams were performed without a DUT to determine the intrinsic resolution power, sensor efficiencies and noise rates for the telescope itself. The assembly of the telescope will be introduced in Chapter 3, the required data acquisition and data analysis software will be shortly introduced in Sections 3.2 and 3.3. The results concerning the SPS test beam analysis towards mechanical stability and efficiency are presented in Chapter 5.

2 Test Beam

2.1 DESY II

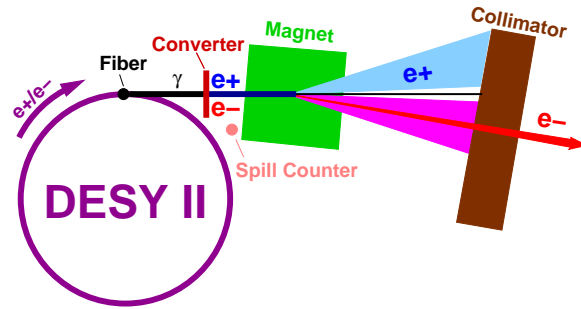


Figure 1: Sketch of test beam production at DESY II.

The DESY test beam is provided by the DESY II storage ring [3]. A sketch of the production mechanism can be seen in Fig. 1. The electron test beam is produced by inserting a target (carbon fiber) into the DESY II electron beam. In the target photons

¹This telescope is placed at the CERN SPS test beam facility. A copy of this telescope is the ANEMONE telescope which is currently placed at the DESY test beam facility.

3 The EUDET Telescope

are created via Bremsstrahlung of the impinging electrons. The photons are then converted to electron-positron pairs. With the help of a magnet one can then choose the negative charged electrons and direct them onto the collimator which focuses the beam. By adjusting the magnet current the energy of the electron beam can be varied between 1 GeV and 6 GeV or even up to 7 GeV.

2.2 SPS

The SPS beam at CERN is produced similarly. There pion beams are created by inserting a target into the proton beam. This pions then can be used as a test beam with energies between 20 GeV and 180 GeV.

3 The EUDET Telescope

The EUDET pixel telescope consists of six sensorplanes and two arms where each supports three of the sensorplanes [4]. In between these two arms is space for the positioning of the DUT. The six sensorplanes are equipped with Mimosa26 sensors. These sensors are Monolithic Active Pixel Sensors (MAPS), where Mimosa stands for Minimum Ionizing particle MOS Active pixel sensor. The Mimosa chips have an active surface of 1152×576 pixels, thus in total $663\,552$ pixels, and with a pixel pitch of $18.4\,\mu\text{m}$ this gives an active area of $21.2 \times 10.6\,\text{mm}^2$ [1]. Also zero suppression is done on the sensor chips. The thickness of the sensors is $50\,\mu\text{m}$. While operating the telescope in the test beam the sensors are kept at a constant temperature of 14°C .

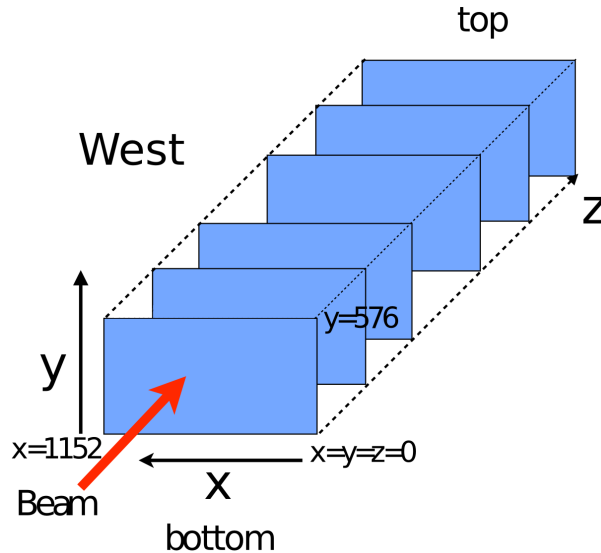


Figure 2: Geometry of the pixel telescopes (DESY test beam).

3 The EUDET Telescope

Figure 2 illustrates the geometry of the telescope placed at the DESY test beam area with the coordinate system, where the beam direction coincides with the positive z -axis direction.

3.1 Experimental Setup

Figure 3 shows the ANEMONE telescope at the DESY test beam. The test beam first impinges on sensor 0 and then passes the other planes with sensor 1, 2, 3, 4 and 5. As mentioned above, the z -axis points along the beam direction whereas the x -axis points horizontally (at DESY to the west) and the y -axis vertically upwards. The measurements with EUDET and ANEMONE were performed with the same geometry for both telescopes. On each telescope arm the sensors have a distance of 10 cm and the space between the two arms is 20 cm. The measurements were performed without a DUT. Throughout all measurements the geometry has not been changed.

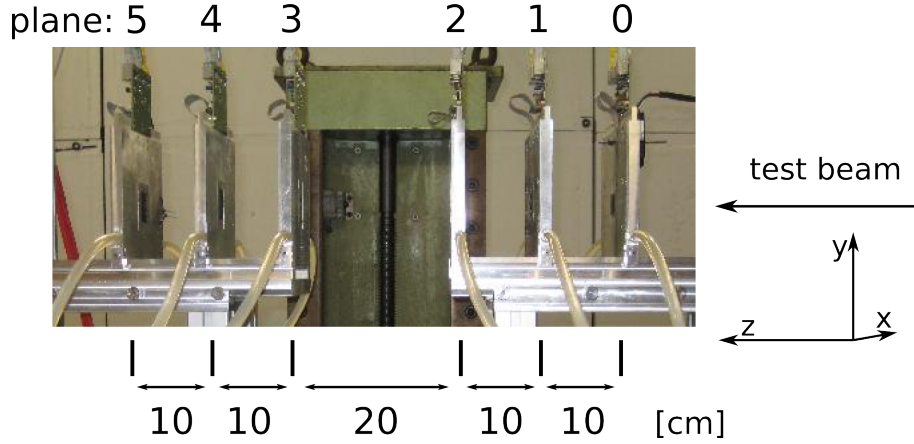


Figure 3: Geometry of the ANEMONE telescope (same geometry as EUDET).

3.2 EUDAQ Software

The EUDAQ software is the data acquisition software of the pixel telescopes. It is a custom designed software that is modular and portable [2]. Figure 5 gives an overview of the ingredients of the EUDAQ system. There are different 'producers' that are programmes that are connected with each other via the network. One of the producers is the 'Trigger Logic Unit' (TLU). The telescope is surrounded by two trigger scintillators on each site. The inputs from the four triggers can be combined to any kind of (anti-)coincidences to generate a trigger signal. The TLU can then produce event numbers and time stamps which are read out via USB by a secondary PC that is placed in the test beam area and also steers the sensor programming. The pixel sensors are read out by custom made reduction boards, which are called EUDRB (EUDET Reduction Board). The data is sent to the VME readout and from there via Gigabit Ethernet to the main EUDAQ PC in the control room. The different producers are connected to the

3 The EUDET Telescope

'Run Control' which controls the whole DAQ system. The connected 'Data Collector' receives the data streams from the producers and then builds the events and stores the data on an storage device. Also available in the EUDAQ software is an 'Online Monitor' which creates histograms while taking the data and enables data quality checks online. One of these quality checks is the control of correlation plots. Correlation plots show the distribution of the X and Y hit-coordinates of a particular sensor as functions of these coordinates of a different sensor. One gets two-dimensional histograms which are expected to show a diagonal line from the lower left corner to the upper right corner (see for example Figure 4). At DESY multiple scattering of the impinging electrons can cause slightly smeared lines. Also provided in the software is a 'Log Collector' that collects all log-messages from the producers.

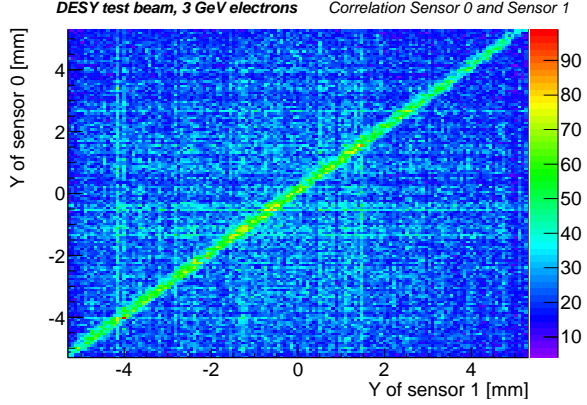


Figure 4: Correlation of Y hits in sensor 0 and Y hits in sensor 1. For small distances between planes and small multiple scattering angles the shown behaviour is expected.

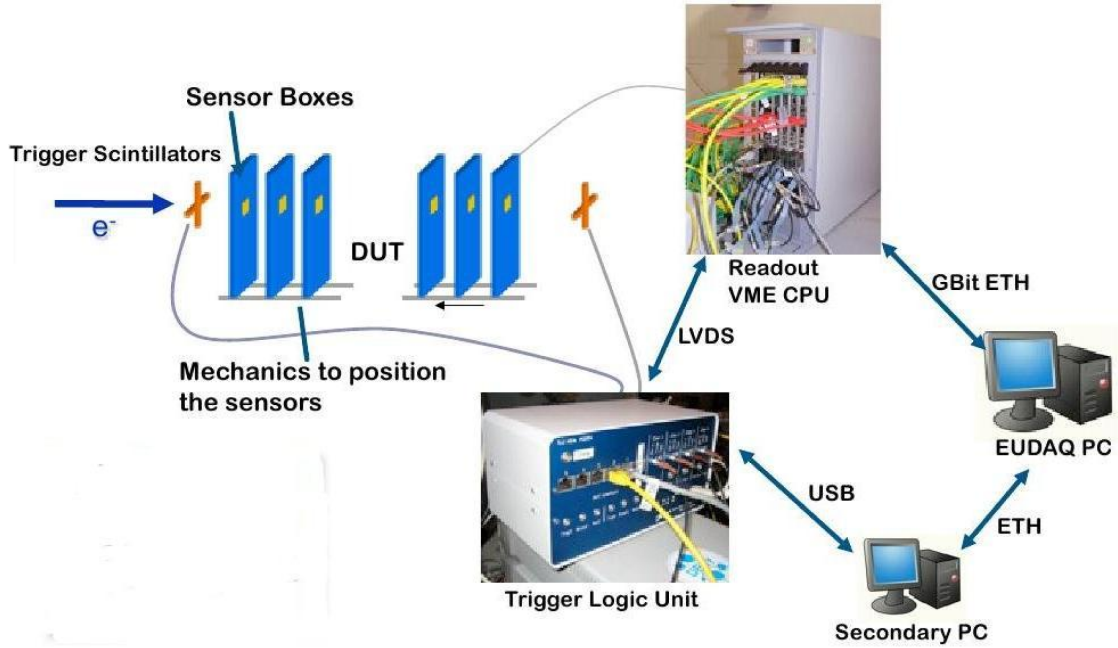


Figure 5: Sketch of the DAQ system of the EUDET telescope.

3.3 EUTelescope analysis software

After the data taking and storage by the EUDAQ software the data-files have to be analyzed which is done by the EUTelescope software. The goal of the software is to reconstruct the tracks that passed the telescope from raw data acquired. The EUTelescope software is based on MARLIN and LCIO data format [5]. MARLIN is an analysis framework written for projects aiming towards the future international linear collider (Modular Analysis & Reconstruction for the LIN collider).

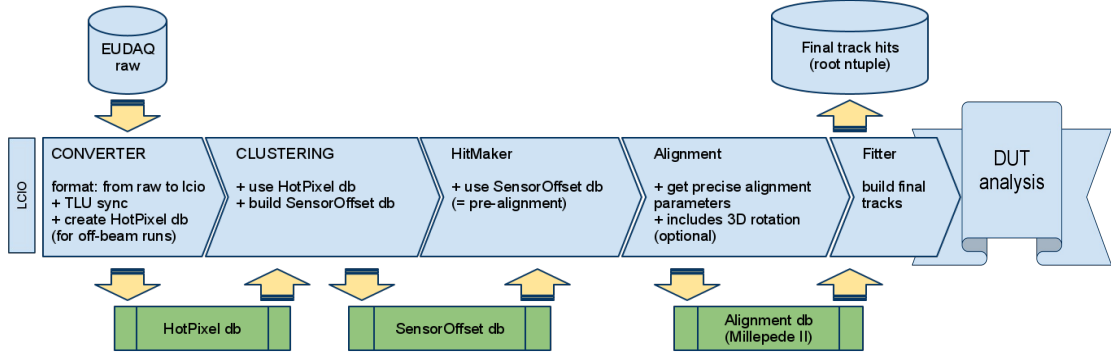


Figure 6: Illustration of the used different reconstruction steps in the data analysis.

After receiving the raw data-file format from the EUDAQ the EUTelescope is operated basically in five steps. The current analysis chain used, is depicted in Figure 6. In The following the five steps of the analysis will be explained.

3.3.1 Conversion

The first step in the EUTelescope analysis chain is the conversion of the raw data-formats into the LCIO data-formats, which is necessary for the next analysis steps to work.

3.3.2 Clustering

After that a clustering algorithm tries to group pixel hits to a cluster. A cluster is a group of adjacent pixels that have fired. A pixel fires when the produced voltage-signal lies over a certain threshold. Thus a threshold is the amount of voltage above which pixels fire. When a particle passes through the sensor it can cause more than one pixel to fire and therefore several pixels report a hit. The clustering algorithm groups these pixels together to one hit, where the particle passed the sensor.

3.3.3 Hitmaker

After clusters are found by the clustering algorithm the hitmaker tries to define the hit position in the cluster which is the most central pixel of the cluster. The criteria for the most central pixel contain the number of adjacent pixels and the distance of the pixel to

3 The EUDET Telescope

the cluster border. The lower the threshold, the more pixels fire when a particle passes through. Thus it is easier to reconstruct the hit position of larger clusters. For high thresholds the cluster sizes are small and therefore finding the most central hit is more difficult. So obviously these threshold settings have an impact on the intrinsic sensor resolution.

3.3.4 Alignment

The fourth step of the analysis chain is the alignment. The imperfections of the mechanical alignment of the six sensor planes to each other have to be corrected. This is done on software basis via the Millepede II programme. The alignment uses a quick track fitter which identifies sensor hits belonging to the same track. This information is used to determine certain alignment parameters. The pixel telescopes are sensitive to three of these alignment parameters: a shift in x - and y -direction and a rotation in the x, y -plane, which are denoted by X , Y and the angle γ . Fig. 7 shows these three parameters that correct the sensor positions. The sensitivity to rotations around the x - and y -axis is less because the beam is impinging perpendicular onto the telescope.

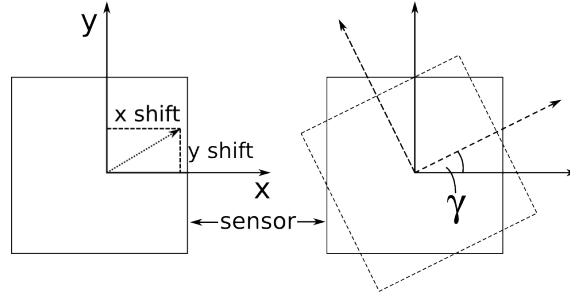


Figure 7: Illustration of the three alignment parameters

In the analysis the alignment is done by fixing plane 0 and aligning the other planes with respect to this one. Therefore the alignment parameters for plane 0 are all 0.

3.3.5 Track-Fitting

The final step is the track-fitting which uses the information from the hitmaker and the alignment analysis. The track fit uses a χ^2 -minimization that accounts for multiple scattering of the impinging particle. The distribution of the scattering angle θ_i for plane i is assumed to be Gaussian with a width of [6]:

$$\Delta\theta_i = \frac{13.6 \text{ MeV}}{\beta c p} q \sqrt{\frac{dx}{X_0}} \left[1 + 0.38 \ln \left(\frac{dx}{X_0} \right) \right].$$

This width depends on the velocity βc , the momentum p and the charge q of the incident particle, where dx/X_0 is the thickness of the scattering material in radiation lengths (in this case the radiation length for silicon is $X_0^{\text{Si}} = 9.36 \text{ cm}$). Figure 8 illustrates the

4 Measurement

scattering angles in x - and y -direction and the relation to the measured hit position and the fitted hit position in the sensor. The angles are assumed to be small, and therefore [7]:

$$\theta_x^i \approx \frac{x_{\text{fit}}^{i+1} - x_{\text{fit}}^i}{z^{i+1} - z^i}, \quad \text{analogue for } \theta_y^i.$$

The χ^2 from the fit in the x, z -plane is then:

$$\chi_x^2 = \sum_{i=1, i \neq i_{\text{DUT}}}^N \left(\frac{x_{\text{fit}}^i - x_{\text{meas}}^i}{\sigma_i} \right)^2 + \sum_{i=2}^{N-1} \left(\frac{\theta_x^i - \theta_x^{i-1}}{\Delta\theta_i} \right)^2. \quad (1)$$

No correlations are assumed between horizontal and vertical position measurements and therefore the track fitting in x - and y -direction is independent. The fit is done for each sensor separately. The considered sensor is treated as DUT (position of DUT: i_{DUT}) and hits are required in all other 5 sensors to form a track ($N=6$, total number of sensors). The first term in 1 is due to the uncertainty (σ_i) of the hit position measurement and the second term is the one that takes multiple scattering into account. No scattering angles can be determined for the first and the last plane. Finding the minimal χ^2 is equivalent to solving a set of linear equations and can be done analytically (see [7]). The width of the distribution of $x_{\text{fit}} - x_{\text{meas}}$ (measured residuals) gives the measured resolution which is needed for determining the intrinsic resolution of the sensor and the pointing resolution. The relations between these terms and the determination is described in [8] and [9]. Results from our test beam measurements concerning the intrinsic sensor resolution and the pointing resolution are presented in [10].

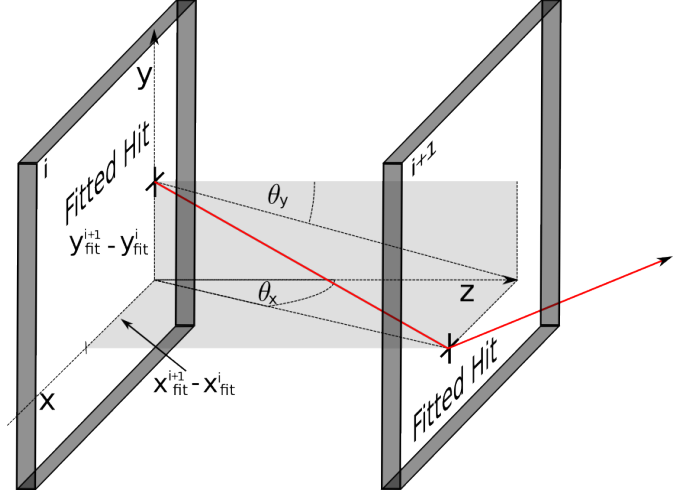


Figure 8: Multiple scattering angles between two planes i and $i+1$.

4 Measurement

Measurements with the pixel telescopes alone have been performed at the CERN SPS test beam and at the DESY test beam.

4.1 Test Beam Measurement at the CERN SPS Storage Ring

The measurements with the EUDET telescope at SPS have been performed in a time period of 14 days from 08.08.2011 to 21.08.2011. The data were taken remotely. In

this time no one should have touched the telescope. The measurements were done with a pion test beam with 120 GeV. Few measurements with 80 GeV were also performed. For the 120 GeV pions a threshold scan from threshold 5 to 10 in whole steps has been conducted. For each threshold about two million events were recorded in order to get a sufficient statistic. Due to the conditions at the SPS storage ring, beam was for about 10 seconds in one minute available. The triggers did not cover properly the active sensor area and therefore these were moved at 10.08.2011. The test beam set up was changed on 12.08.2011, which changed the hit rate and the beam geometry. There were problems with double correlations before. The higher hit rate caused a large number of tracks per event (up to 8, 9 tracks). There were also data taken at threshold 4 but yet not analyzed. Measurements without test beam were performed for all thresholds from 4 to 10 as well.

4.2 Test Beam at DESY II

Test beam measurements with ANEMONE alone at DESY II were performed in a period of 17 days from 10.08.2011 to 26.08.2011. A threshold scan from 5 to 10 has been done for electrons of energy 2 GeV, 3 GeV and 4 GeV. Due to the high hit rate at the DESY II test beam, data with 5 or 10 million events for every threshold of each energy were taken. This data has not been analyzed yet.

5 Results

5.1 CERN Test Beam

In the following results from the analyzed SPS data concerning the mechanical stability of the telescope and the efficiency of the telescope sensors are presented.

5.1.1 Alignment Parameters - Mechanical Stability

One of the aims of the test beam measurements was to prove the mechanical stability of the telescope. Apart from moving parts of the telescope, which should not have happened during the data taking period, influences on the alignment parameters, which are a measure for the mechanical stability, are possibly the changing temperature in the SPS test beam hall, vibrations and changed test beam set ups.

To test the mechanical stability plots were made which show the three introduced alignment parameters X , Y and γ as a function of time. These plots are shown in Figure 9. The plots on the left site show the alignment parameters for sensors 1 to 5 as a function of time. In these plots the absolute values for X , Y and γ are shown. Sensor 0 was fixed and therefore the alignment parameters are 0 for this sensor and are not shown. One observes that the X and Y parameters for sensor 2 are very close to zero and therefore this sensor seems to be already mechanically closely aligned to sensor 0. To get a better impression of the deviations of the single parameters of each sensor the plots on the right site of Fig. 9 were created. They show the same values where the first value for all sensors was subtracted from all other values, thus the plot is normalized to the first value, which

5 Results

lies at 0. The deviations over the whole period of 14 days lie in a range of 15-20 μm for X and Y and γ deviations are in a range of about 25 mrad. One can also observe that the deviations for planes which are further away from the first planes are generally larger than the others which is expected because of the alignment with respect to the first plane. The last values in the plots for 21.08.2011 are in fact values obtained from the 80 GeV pions measurement.

The deviation plots show a first jump at 10.08. which is probably caused by a movement of the scintillators (see Sect. 4.1). A next jump is visible at 12.08. The reason for this might be a change in the test beam set up which could have had an impact on the beam geometry and therefore affect the alignment as well. Then one observes a rather constant period until 14.08.2011.

For this period we have no knowledge of any interruption or changed test beam conditions. In Fig. 10 this period is shown, where again the first value of this period was subtracted from all other values for each sensor. The deviations are now in a range of about 6 μm . In the X and γ alignment parameters there is a drop from 13.08 to 14.08. visible. It is yet not clear where this might come from.

5 Results

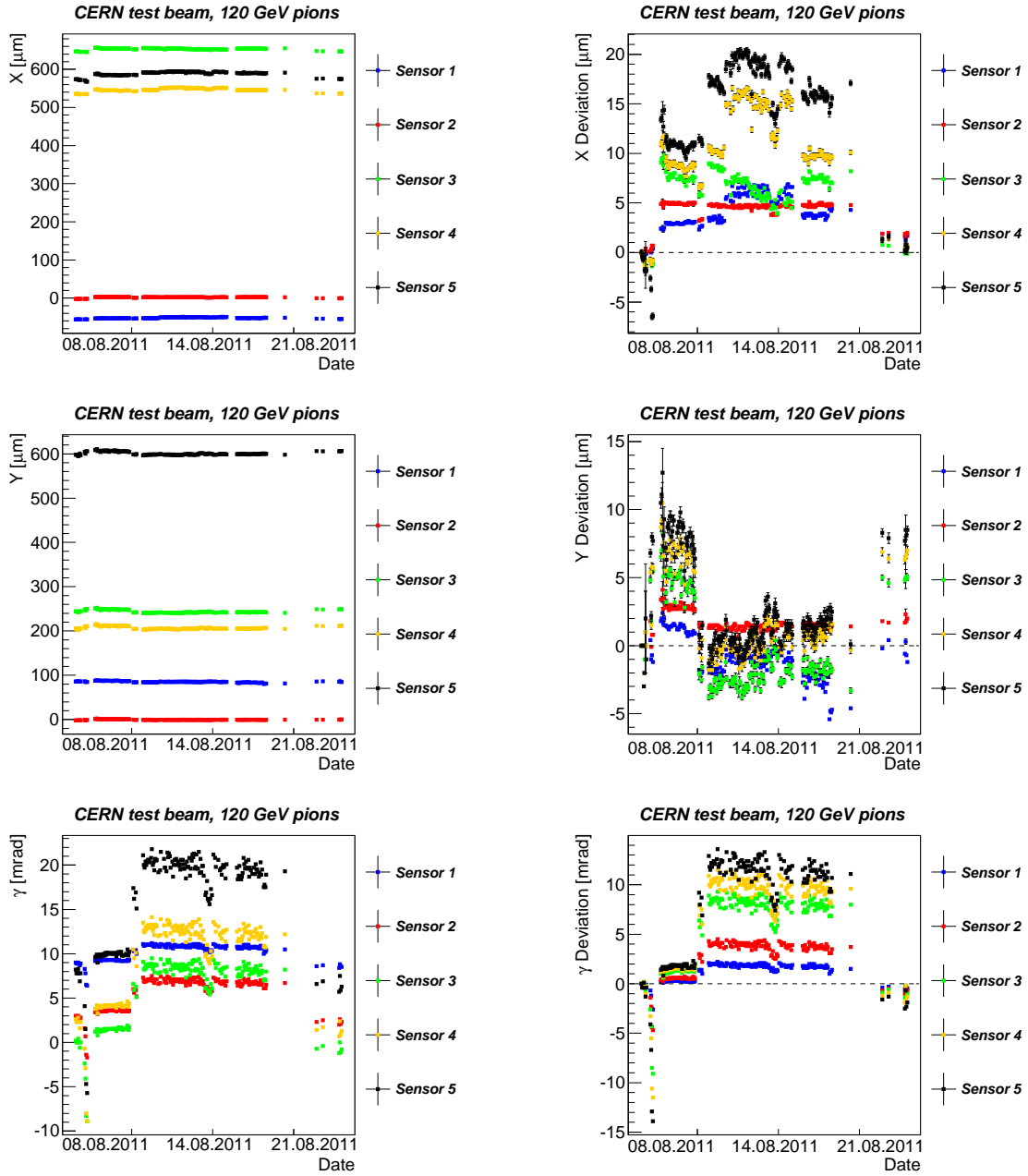
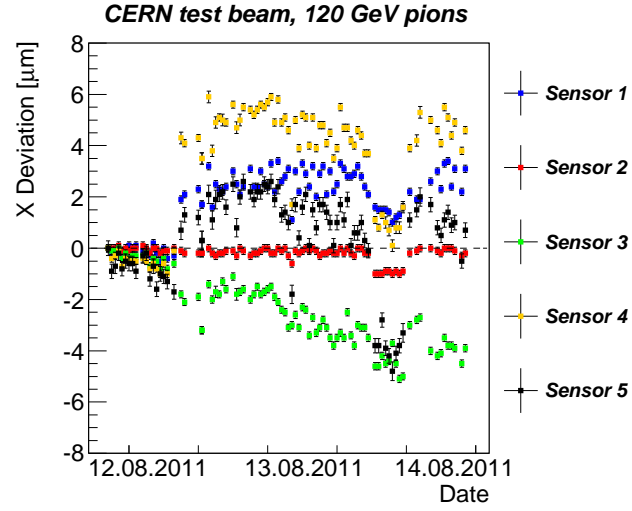
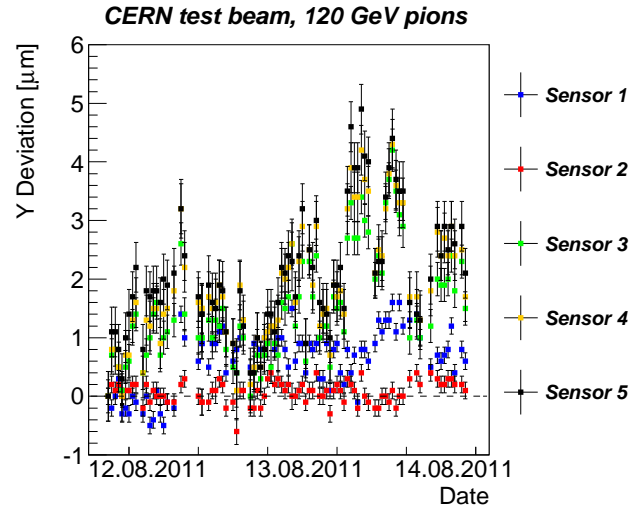


Figure 9: Alignment parameters X , Y and γ as functions of the time. Left: absolute values, right: first value subtracted from all other values for each sensor. Entries from 21.08.2011 belong to the 80 GeV measurements.

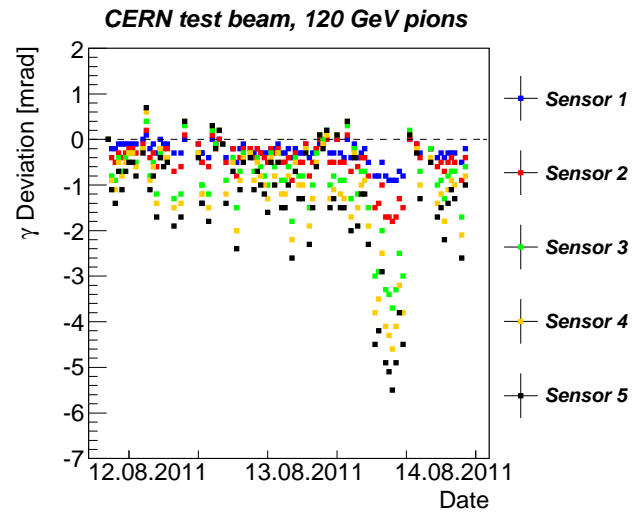
5 Results



(a)



(b)



(c)

Figure 10: Deviation of X (a), Y (b) and γ (c) parameter in period from 12.08–14.08.2011. The first value from this period was subtracted from all other values for each sensor.

5.1.2 Efficiency

Another aim of the test beam measurements was to determine the efficiency of the individual sensors. The efficiency is defined as the fraction of actual tracks that are detected by the individual sensors. Or in other words it is a probability to detect a track if there actually has been a particle passing the sensors. In contrast to that, the fake hit rate is the probability of detecting a track when there was no test beam particle passing caused by electronic noise or e.g. cosmic muons (the fake hit rate was determined by measurements without test beam and is presented in [11]).

The efficiency was estimated by the following expression:

$$\text{Efficiency} = \frac{\# \text{ of matched hits}}{\# \text{ of fitted hits}} \quad (2)$$

The fitted hit is the fitted track position in the sensor, where we only look at the center of the sensor to ensure, that we do not choose a fitted position that is outside the active sensor area. A matched hit is a hit position that is matched to a fitted track position. It is matched when the distance between the hit position and the fitted position is smaller than a certain value R_{max} . In our case this value is $R_{\text{max}} = 1$ mm.

Figure 11 shows the comparison of two efficiency-maps for sensor 0 for thresholds 5 and 10. In the plot for threshold 5 one can see the trigger window that did not fully cover the depicted area of the sensor. This can also be seen for threshold 10 at the top margin, where meanwhile the trigger scintillators have been moved and therefore the window covered almost the whole range. The bin width in both plots is $20 \mu\text{m}$ in x - and y -direction which is chosen because it is close to the pixel pitch of $18.4 \mu\text{m}$. For threshold 5 the efficiency lies almost everywhere close to one, where the efficiency decreases for higher thresholds which can be clearly seen for threshold 10. This behaviour is expected because it is more likely to lose tracks for requirements of higher voltage signals, thus for higher thresholds.

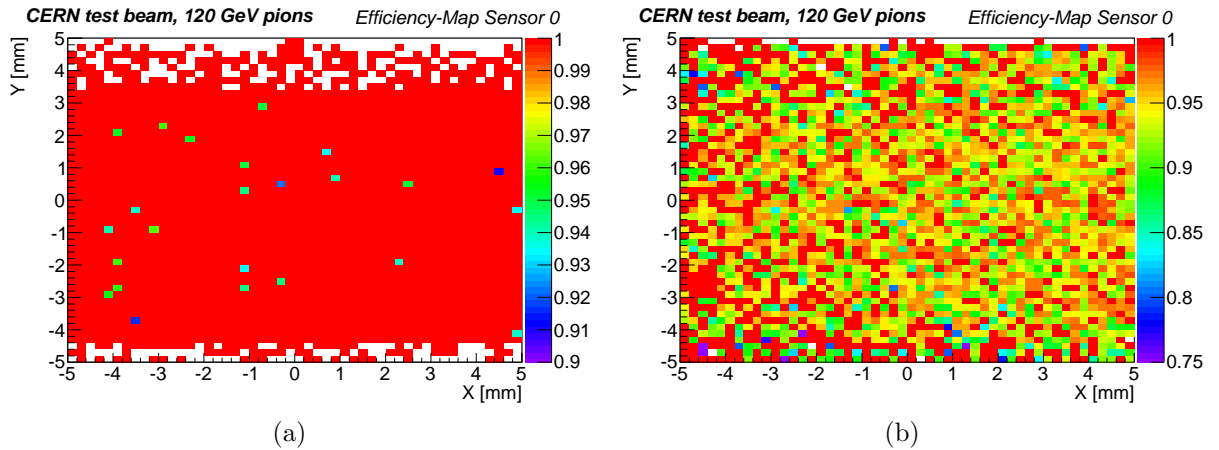


Figure 11: Efficiency-map of sensor 0 for threshold 5 (a) and threshold 10 (b). The trigger scintillators have been moved during the data taking, therefore the range covered by the trigger is different for both thresholds.

5 Results

The efficiencies determined after Equation 2 were plotted as a function of the threshold for 120 GeV and 80 GeV pions as well. The errors on the efficiency were calculated for each run² by assuming poissonian errors³ on '# of matched hits' and '# of fitted hits' and conducting error propagation⁴. The values for all runs in total per threshold were obtained by calculating the weighted mean. The plots are shown in Fig. 12. There were only few measurements with less numbers of events performed with 80 GeV pions and only analyzed for thresholds 5, 6 and 8. Therefore the uncertainties on the efficiencies are larger than the uncertainties for the 120 GeV measurement. The behaviour of the efficiency for sensor zero follows the expected behaviour. In both plots all other sensors show an unexpected behaviour. The efficiencies are all close to 100% and then suddenly drop off at threshold 10 to a lower value, especially the value for sensor 5. In principle all sensors should behave the same and should have similar efficiencies. In reality this is not the case because every sensor consisting of four readout submatrices is unique and therefore shows slightly different values. But the values seen in the plot cannot be explained by this.

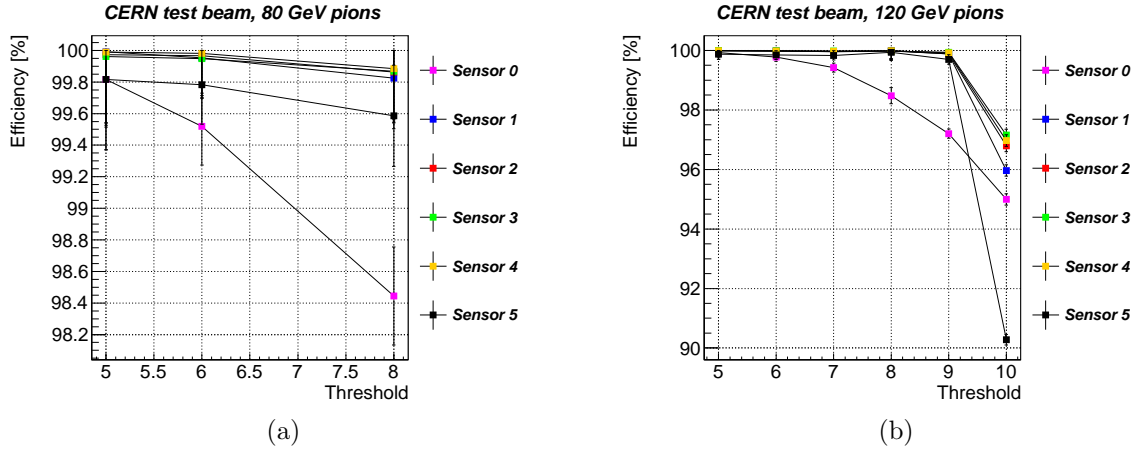


Figure 12: Efficiency as a function of the threshold for 80 GeV (a) and 120 GeV pions (b).

5.2 Common Result

The goal of determining the threshold dependencies of the intrinsic sensor resolution, the efficiency and the fake hit rate is to determine the best threshold setting for test beam operation. The requirements are a high efficiency very close to 100%, the highest possible resolution and the lowest possible fake hit rate. These requirements cannot be fulfilled at the same time, but one can find a compromise. Figure 13 shows the graphs of all these quantities (only for sensor 0) in one plot which reflects the work of us three summer students working on the EUDET telescope. The task is now to interpret this plot in terms of finding the best threshold setting.

²A run is completed after triggering an amount of events which corresponds to a file size of ≈ 1 GB.

³Which is reasonable because of the large numbers for each quantity.

⁴See a different approach in the Appendix A.

6 Summary and Conclusion

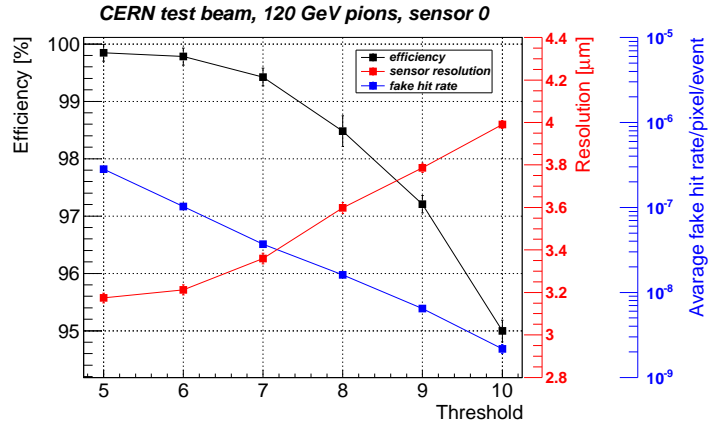


Figure 13: Efficiency, intrinsic resolution and fake hit rate as functions of the threshold.

6 Summary and Conclusion

Test beam measurements with the EUDET and ANEMONE telescope have been successfully performed. The data taken with EUDET have been analyzed and results concerning the mechanical stability of the telescope and efficiency measurements of the sensors have been presented here. The telescope has been proven to be stable over a period of 14 days. The deviations in the alignment parameters are only caused by micrometer effects. There are a few jumps in the alignment graphs that can be partly explained by movement of scintillators and changed test beam settings. Deviations from 13.08. to 14.08 cannot certainly be explained. It might be that temperature changes in the test beam hall from day to night influence the telescope alignment. But this is just one possible explanation and has to be clarified with future measurements where the temperature of the test beam hall is also recorded.

The efficiency behaviour as a function of the threshold for sensor 0 is as expected. An assumed bias in the fitter step has been confirmed by the plot of the efficiency for the other sensors. This is a bug that has to be found in the track fitting and might also have effects on other measured quantities.

Future steps are to analyze the data taken with ANEMONE in the DESY test beam. Statistical uncertainties will be lowered due to the large amount of data that was taken. Also dependencies on the particle type and the energy of the test beam particles can then be investigated as well as the effect of multiple scattering on the measurement.

Acknowledgement

I would like to thank our supervisor Ingrid Gregor for her kind welcome in her group and for helpful discussions of results and creating an atmosphere where it was a pleasure to work in. Also many thanks to Igor Rubinsky who finally became our second supervisor;). Thank you for all your time consuming efforts helping us with the analysis, fixing bugs

6 Summary and Conclusion

and discussing achieved results. I would also like to thank Marcel Stanitzki and everyone else in the group who helped us with our work. I also want to express my gratitude to Olaf Behnke, Doris Eckstein and Andrea Schrader for organizing the summer students programme giving us the wonderful opportunity to work and live in such a unique environment for this time. Thanks to all the summer students 2011!

A Efficiency Calculation

The results concerning the efficiency of the individual sensors are presented in Section 5.1.2. The approach to calculating the values and the errors is described there. Also another approach has been taken into consideration. One has to take care that the errors on the efficiency cannot exceed 100%. Therefore the errors were cut off at this value in the plots in Figure 12. This may not be a satisfactory treatment of the errors. The `TEfficiency` class in Root provides a solution for this problem [12]. Therefore the means of '# of matched hits' = n_+ and '# of fitted hits' = n were calculated for all runs by calculating the weighted means. These values were then put into one-dimensional histograms. The `TEfficiency` class uses the information in these two histograms for n_+ and n and divides these two to get the efficiency $\epsilon = n_+/n$. Another possibility is to weight different runs. Then for every single run a `TEfficiency` class is created that receives a weight according to the number of reconstructed tracks, in this case n , which is the only difference between the runs in terms of weighting. One can then merge these different classes to one `TEfficiency` class. In this class asymmetric errors are calculated. These errors are determined differently for different methods, i.e. for frequentist approaches and bayesian approach and different confidence levels. The default determination calculates the Clopper-Pearson interval (frequentist approach) for the efficiency ϵ with a given confidence level of $1 - \alpha$ (0.683) according to:

$$P(X \geq n_+, \epsilon, n) = \frac{\alpha}{2} \quad \text{and} \quad P(X \leq n_+, \epsilon, n) = \frac{\alpha}{2}. \quad (3)$$

P is the binomial probability for the true efficiency ϵ to get n_+ events, where the total number is n (see Eq. 4). The asymmetric errors are **error high** for the upper boundary of ϵ , which is the $1 - \alpha/2$ quantile and **error low** for the lower boundary, which is the $\alpha/2$ quantile of P . The new plots for this calculation are shown in Figure 14

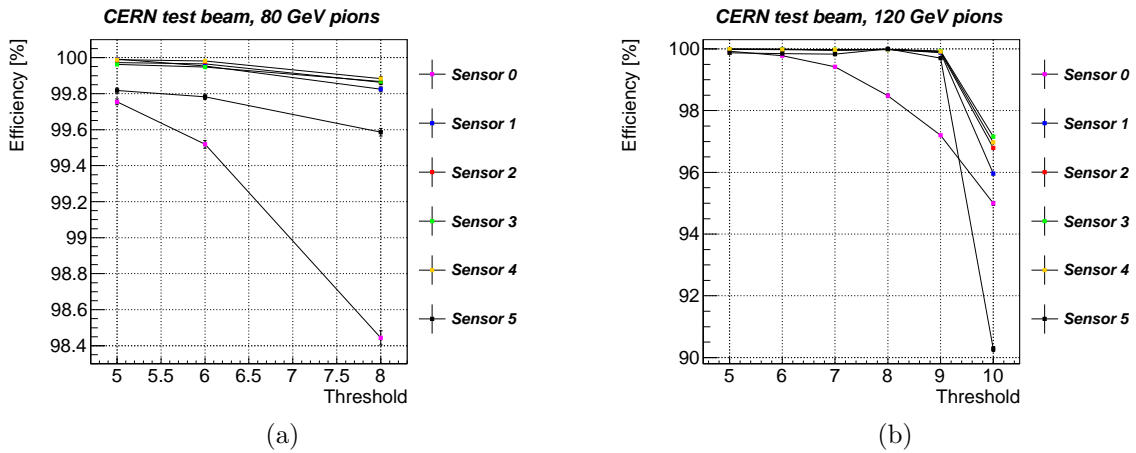


Figure 14: Efficiency as a function of the threshold for 80 GeV (a) and 120 GeV pions (b) created by using `TEfficiency` calculation in Root.

A Efficiency Calculation

The errors are smaller than before and are more likely to describe the uncertainties correctly.

Calculation using Binomial Errors

The errors on the efficiency ϵ can be calculated by assuming n_+ to be binomially distributed with n fixed [13]:

$$P(n_+, n) = \binom{n}{n_+} p^{n_+} (1-p)^{n-n_+}. \quad (4)$$

p is the true efficiency and taking ϵ as the estimate for p leads to the following formula using the known variance V_p of a binomial distribution $V_p = np(1-p)$:

$$\sigma_\epsilon = \sqrt{V_\epsilon} = \sqrt{\frac{1}{n^2} V_p} = \sqrt{\frac{n_+ n_-}{n^3}} = \sqrt{\frac{\epsilon(1-\epsilon)}{n}}, \quad (5)$$

where $n_- = n - n_+$. The relation $\sigma_\epsilon = \frac{1}{n} \sigma_p$ for the estimator of the standard deviation σ_ϵ is taken into account, because we do not know the true efficiency p . With Equation 5 one can show that the following conditions are fulfilled:

$$\begin{aligned} \epsilon - \sigma_\epsilon &\geq 0 \\ \epsilon + \sigma_\epsilon &\leq 1. \end{aligned}$$

By comparing the symmetric errors calculated with this approach (**error calc** in following plots) and calculated by the TEfficiency class one sees that σ_ϵ coincides with **error high** (see Fig 15). The values for **error low** are always larger.

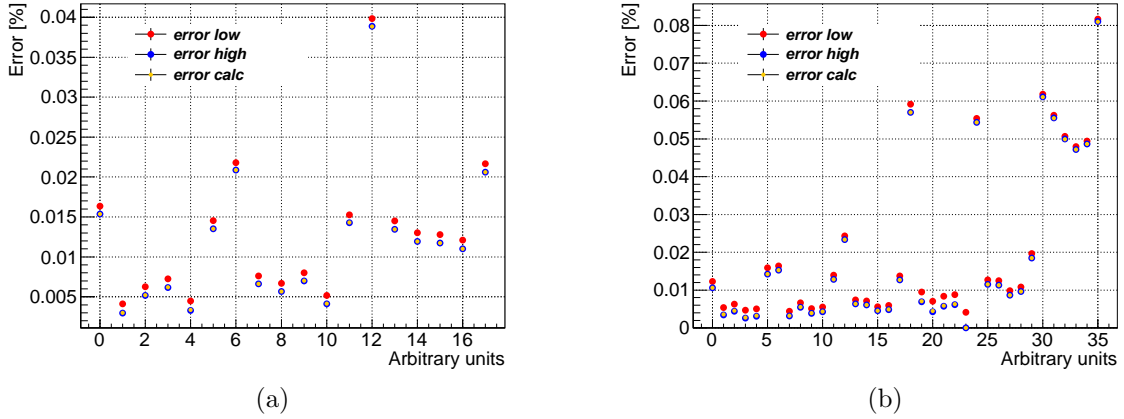


Figure 15: Errors of the efficiency for 80 GeV (a) and 120 GeV pions (b) and different calculations.

Thus it seems that the error calculation of Equation 5 is equivalent with calculating the upper boundary **error high** of the Clopper-Pearson interval used by TEfficiency. The lower boundary **error low** is calculated differently according to the determination in Eq. 3.

References

- [1] I.-M. Gregor, *The EUDET Telescope - at DESY and CERN*, Talk, CERN Detector Seminar, Geneva (2010)
- [2] EUDET, *Detector Research and Development towards the International Linear Collider* (2010)
- [3] T. Behnke, E. Garutti, I.-M. Gregor, T. Haas, U. Kötz, I.-A. Melzer-Pellmann, N. Meyners, J. Mnich, F. Sefkow, *Test Beams at DESY*, EUDET-Memo-2007-11 (2007)
- [4] A. Bulgheroni, *First Test Beam Results from the EUDET Pixel Telescope*, EUDET-Report-2007-06 (2007)
- [5] EUTelescope software documentation webpage: URL <http://projects.hepforge.org/eudaq/Eutelescope/intro.html>
- [6] V. L. Highland, Nucl. Instrum. Methods 129:497 (1975)
- [7] A. F. Zarnecki, P. Niezurawski, *EUDET Telescope Geometry and Resolution Studies*, EUDET-Report-2007-01 (2007)
- [8] A. Bulgheroni, *Results from the EUDET telescope with high resolution planes*, EUDET-Report-2009-02 (2009)
- [9] J. Behr, *Test Beam measurements with the EUDET Pixel Telescope*, EUDET-Report-2010-01 (2010)
- [10] S. Kuttimalai, *Test Beam Measurements with Pixel Telescopes - Intrinsic Resolution*, DESY Summer Students Programme Report (2011)
- [11] I. Khvastunov, *EUTelescope - Adding a data base to make life easier*, DESY Summer Students Programme Report (2011)
- [12] TEfficiency class, Root documentation webpage: URL <http://root.cern.ch/root/html/TEfficiency.html>
- [13] B. List, *Statistical Errors of Efficiency Determination from Weighted Events* (1999)